Beampattern Synthesis With Dynamic Range Ratio Constraint via Sequential Convex Optimization

Lingrui Li, Xuejing Zhang, *Member, IEEE,* Zishu He, *Member, IEEE*

***Abstract*—In this paper, we consider beampattern synthesis with a constraint on the dynamic range ratio (DRR), which is defined as the proportion between the maximum and minimum amplitude excitations applied to the array elements. Utilizing the trigonometric function technique, we reformulate and simplify the non-convex constraint on DRR. This allows us to derive a new beampattern synthesis formulation with DRR constraint, which can be solved through sequential convex optimization. Compared to existing algorithms, the proposed algorithm can be executed very easily. Moreover, our algorithm exhibits high effectiveness on both focused and shaped beampatterns. Both theoretical and simulation results confirm that the proposed algorithm does not rely on the initial setting and exhibits good convergence performance. Representative simulations are provided to demonstrate the effectiveness and superiority of the proposed algorithm in various scenarios.**

***Index Terms*—Beampattern synthesis, dynamic range ratio constraint, focused beampattern, shaped beampattern, convex optimization.**

I. Introduction

BEAMPATTERN synthesis has attracted significant attention in recent years due to its diverse applications in radar, communication, and other fields. Various algorithms have been proposed for beampattern synthesis, including global search algorithms [1]–[3], deterministic algorithms [4]–[6], and optimization algorithms [7]–[11]. Nevertheless, a crucial consideration in practical array systems is the dynamic range ratio (DRR), which is defined as the proportion between the maximum and minimum amplitude excitations applied to the array elements. A high DRR leads to a substantial increase in costs. This is primarily due to the fact that antennas with higher DRR typically require more complex and expensive hardware components. Therefore, beampattern synthesis with DRR constraint is crucial in designing cost-efficient antenna array systems.

In previous works, a number of strategies haven been proposed to reduce DRR in beampattern synthesis. In [12], the DRR suppression was discussed with null constraints. The authors showed that the lower bound of the DRR depends on the null directions. However, this method can be computationally intensive when strict constraints are applied. The semidefinite relaxation technique was utilized in [13] to reduce DRR. However, it required an approximate eigenvalue decomposition [14] to recover the excitations, which may degrade the performance of beampattern. An iterative approximation algorithm was presented in [15] to reduce DRR, by approximating the non-convex DRR constraint as a linear convex one. Since an additional correction to the weights is required, the beampattern may be deteriorated ultimately. In [16], auxiliary variables were incorporated to enforce the excitations to comply with the DRR. Similar to [15], an additional correction is required for the algorithm in [16]. The authors of [17] proposed a depth-first algorithm to constrain DRR in case of real excitations. However, it is unable to independently solve the shaped beampattern synthesis problem with DRR constraint. Apart from the aforementioned works, there are other algorithms proposed to reduce DRR as reported in [18]–[24]. All the aforementioned algorithms suffer from several issues, including slow convergence rates, resulting high DRRs, and unsatisfactory beampatterns.

In this paper, we consider beampattern synthesis with DRR constraint. Utilizing the trigonometric function technique [25], we reformulate and simplify the non-convex constraint on DRR. This allows us to derive a new beampattern synthesis formulation with DRR constraint, which can be solved through sequential convex optimization. Compared to existing algorithms, the proposed algorithm can be executed very easily. Moreover, our algorithm exhibits high effectiveness on both focused and shaped beampatterns, while demonstrating insensitivity to the selection of initial parameters for iterations. Representative simulations are conducted to show the effectiveness and superiority of the proposed algorithm.

II. Problem Formulation

Assuming narrowband and far-field conditions, we take focused beampattern synthesis as an example. The objective is to synthesize a beampattern that radiates main beam towards θ_0, while minimizing the peak sidelobe level (PSL). Considering the DRR constraint, we can formulate the problem as

$$\min_{\boldsymbol{w},\rho} \quad \rho \tag{1a}$$

$$\text{s.t.} \quad \boldsymbol{w}^H \boldsymbol{a}(\theta_0) = 1 \tag{1b}$$

$$|\boldsymbol{w}^H \boldsymbol{a}(\theta_s)| \le \rho,\ \theta_s \in \Theta_S \tag{1c}$$

$$\mathrm{DRR}(\boldsymbol{w}) \le \varepsilon \tag{1d}$$

where $\boldsymbol{w} = [w_1, \cdots, w_N]^T$ is the complex excitation vector, N stands for the element number, $(\cdot)^H$ denotes the Hermitian transpose, $(\cdot)^T$ denotes the transpose operation, ρ stands for the PSL, ε represents the given upper limit for DRR, Θ_S is the sidelobe region, $\boldsymbol{a}(\theta)$ is the steering vector defined as

$$\boldsymbol{a}(\theta) = [g_1(\theta)e^{-j\omega\tau_1(\theta)}, \cdots, g_N(\theta)e^{-j\omega\tau_N(\theta)}] \tag{2}$$

where $g_i(\theta)$ is the element pattern of the ith antenna, ω is the operating frequency, $\tau_i(\theta)$ denotes the time delay between the ith element and the reference one.

In problem (1), the DRR is defined as

$$\mathrm{DRR}(\boldsymbol{w}) \triangleq \frac{\max\limits_{n=1,\cdots,N} |w_n|}{\min\limits_{m=1,\cdots,N} |w_m|}. \tag{3}$$

Then, the DRR constraint (1d) can be readily re-expressed as

$$\frac{\min\limits_{m=1,\cdots,N} |w_m|}{\max\limits_{n=1,\cdots,N} |w_n|} \ge \zeta \tag{4}$$

where $\zeta \triangleq 1/\varepsilon$. The main challenge for the problem (1) is how to address the non-convex constraint (1d) or (4).

This work was supported in part by the National Nature Science Foundation of China under Grant 62101101, in part by the Sichuan Science and Technology Program under Grant 24NSFSC1433, and in part by the Peng Cheng Shang Xue Education Fund under Grant XY2021602. (*Corresponding author: Xuejing Zhang.*)

The authors are with the University of Electronic Science and Technology of China, Chengdu 611731, China (e-mail:202321010741@std.uestc.edu.cn; zhangxuejing@uestc.edu.cn; zshe@uestc.edu.cn).

III. Beampattern Synthesis With DRR Constraint Using Sequential Convex Optimization.

In this section, we reformulate the DRR constraint, and utilize sequential convex optimization to solve the focused beampattern synthesis problem. Moreover, convergence analysis of the proposed algorithm is presented, and extension to the shaped beampattern synthesis scenario is discussed.

A. Focused Beampattern Synthesis With DRR Constraint

Before addressing the focused beampattern synthesis problem (1), it is essential to observe the following equality:

$$\frac{\min\limits_{m=1,\cdots,N} |w_m|}{\max\limits_{n=1,\cdots,N} |w_n|} = \min_{i,j=1,\cdots,N,\ i\neq j} \left|\frac{w_i}{w_j}\right|. \tag{5}$$

According to (5), the DRR constraint (4) can be rewritten as

$$|w_i| \geq \zeta \cdot |w_j|,\ \forall i,j=1,\cdots,N,\ i\neq j. \tag{6}$$

To handle the above constraints, let

$$\alpha_i \triangleq \angle w_i \tag{7}$$

where $\angle(\cdot)$ returns the phase of input complex value, $i=1,\cdots,N$. Then, it is not difficult to express $|w_i|$ as

$$|w_i| = \mathcal{R}(w_i)\cos(\alpha_i) + \mathcal{I}(w_i)\sin(\alpha_i) \tag{8}$$

where $\mathcal{R}(\cdot)$ and $\mathcal{I}(\cdot)$ stands for the real part and the imaginary part of a complex value, respectively. A graphical interpretation for (8) is shown in Fig. 1.

Combining (6) and (8), the DRR constraint can be formulated as

$$\begin{aligned}\mathcal{R}(w_i)\cos(\alpha_i) + \mathcal{I}(w_i)\sin(\alpha_i) \geq \zeta \cdot |w_j|,\\ \forall i,j=1,\cdots,N,\ i\neq j.\end{aligned} \tag{9}$$

Although the constraint has been simplified in form, the above equality implicitly includes the phase constraint (7), and there exists a multiplicative coupling between w_i and α_i. Simultaneously, we observe that for fixed value of $\{\alpha_i\}_{i=1}^N$, the constraint (9) is convex with respect to $\{w_i\}_{i=1}^N$, rendering the beampattern synthesis problem convex as well.

Based on the above principle, we propose to initialize the value of $\{\alpha_i\}_{i=1}^N$ first, then solve the resulting convex optimization problem to obtain the solution $\bar{\boldsymbol{w}}$. Using the obtained $\bar{\boldsymbol{w}}$, we update $\{\alpha_i\}_{i=1}^N$ according to (7) and proceed to the next iteration of convex optimization. The above process is repeated iteratively. Ultimately, the problem of beampattern synthesis with DRR constraint can be solved using sequential convex optimization.

Specifically, in the kth iteration, we solve the following convex optimization problem:

$$\min_{\boldsymbol{w}_k,\rho}\ \rho \tag{10a}$$

$$\text{s.t.}\ \ \boldsymbol{w}_k^H \boldsymbol{a}(\theta_0) = 1 \tag{10b}$$

$$|\boldsymbol{w}_k^H \boldsymbol{a}(\theta_s)| \leq \rho,\ \theta_s \in \Theta_S \tag{10c}$$

$$\begin{aligned}\mathcal{R}(w_{i,k})\cos(\alpha_{i,k-1}) + \mathcal{I}(w_{i,k})\sin(\alpha_{i,k-1}) \geq \zeta \cdot |w_{j,k}|,\\ \forall\ i,j=1,\cdots,N,\ i\neq j\end{aligned} \tag{10d}$$

where $\{\alpha_{i,k-1}\}_{i=1}^N$ are fixed and determined according to the result of $(k-1)$th iteration as follows:

$$\alpha_{i,k-1} = \angle(\bar{w}_{i,k-1}),\ i=1,\cdots,N \tag{11}$$

with $\bar{\boldsymbol{w}}_{k-1} = [\bar{w}_{1,k-1},\cdots,\bar{w}_{N,k-1}]^T$ representing the optimal solution of the $(k-1)$th iteration. Note that in the initialization stage, an initial $\bar{\boldsymbol{w}}_0$ is required which can be determined randomly, and the initial value of $\{\alpha_{i,0}\}_{i=1}^N$ are obtained accordingly. The aforementioned sequential convex optimization process is conducted iteratively until the difference in PSL obtained from two adjacent iterations satisfying $|\rho_k - \rho_{k-1}| \leq \delta$, where δ is a sufficiently small number, ρ_k is the resulting PSL after the kth iteration.

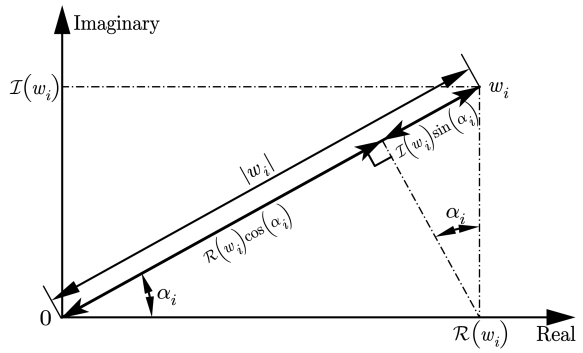

Fig. 1. A graphical interpretation for $|w_i| = \mathcal{R}(w_i)\cos(\alpha_i)+\mathcal{I}(w_i)\sin(\alpha_i)$.

B. Convergence Analysis

Next, we will prove that the value of ρ obtained through the proposed algorithm is monotonically non-increasing with iterations.

To do so, we denote the optimal solution obtained in the $(k-1)$th iteration as $(\bar{\boldsymbol{w}}_{k-1},\ \rho_{k-1})$. Then, $\bar{\boldsymbol{w}}_{k-1}$ and ρ_{k-1} must satisfy

$$\bar{\boldsymbol{w}}_{k-1}^H \boldsymbol{a}(\theta_0) = 1 \tag{12}$$

$$|\bar{\boldsymbol{w}}_{k-1}^H \boldsymbol{a}(\theta_s)| \leq \rho_{k-1},\ \theta_s \in \Theta_S \tag{13}$$

and

$$\begin{aligned}\mathcal{R}(\bar{w}_{i,k-1})\cos(\alpha_{i,k-2}) + \mathcal{I}(\bar{w}_{i,k-1})\sin(\alpha_{i,k-2}) \geq \zeta \cdot |\bar{w}_{j,k-1}|,\\ \forall\ i,j=1,\cdots,N,\ i\neq j.\end{aligned} \tag{14}$$

According to (14), we can further derive that

$$\mathcal{R}(\bar{w}_{i,k-1})\cos(\alpha_{i,k-1}) + \mathcal{I}(\bar{w}_{i,k-1})\sin(\alpha_{i,k-1}) \tag{15a}$$

$$= |\bar{w}_{i,k-1}| \tag{15b}$$

$$\geq |\bar{w}_{i,k-1}|\cos(\alpha_{i,k-1} - \alpha_{i,k-2}) \tag{15c}$$

$$= \mathcal{R}(\bar{w}_{i,k-1})\cos(\alpha_{i,k-2}) + \mathcal{I}(\bar{w}_{i,k-1})\sin(\alpha_{i,k-2}) \tag{15d}$$

$$\geq \zeta \cdot |\bar{w}_{j,k-1}|,\ \forall\ i,j=1,\cdots,N. \tag{15e}$$

Combining (12), (13) and (15), and recalling the optimization problem (10), we know that $(\bar{\boldsymbol{w}}_{k-1},\ \rho_{k-1})$ is a feasible point for the kth iteration. Then, it is evident that

$$\rho_k \leq \rho_{k-1} \tag{16}$$

where ρ_k represents the optimal value for the kth iteration. This indicates that the optimal value of ρ obtained from (10) is monotonically non-increasing with iterations.

C. Extension to Shaped Beampattern Synthesis With DRR Constraint

The proposed algorithm can be extended to the case of shaped beampattern synthesis with DRR constraint. In this scenario, additional non-convex constraints are imposed to limit the lower bound of beampattern level within a specified region Θ_M. After discretizing the angles, the above constraints can be expressed as

$$|\boldsymbol{w}^H \boldsymbol{a}(\theta_m)| \geq l(\theta_m),\ \theta_m \in \Theta_M \tag{17}$$

where $l(\theta)$ denotes the lower bound level.

Utilizing a similar approach to (8), the above constraint (17) can be re-expressed as

$$\mathcal{R}(\boldsymbol{w}^H \boldsymbol{a}(\theta_m))\cos(\beta_m) + \mathcal{I}(\boldsymbol{w}^H \boldsymbol{a}(\theta_m))\sin(\beta_m) \geq l(\theta_m) \tag{18}$$

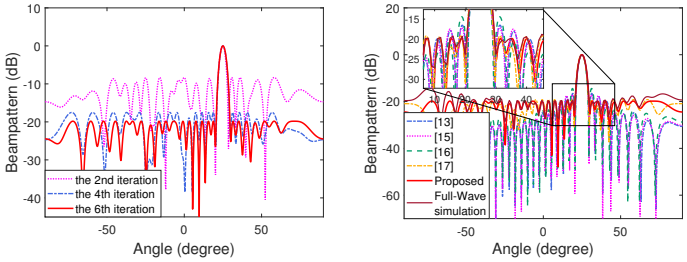

(a) (b)

Fig. 2. Focused beampattern synthesis comparison. (a) Synthesized beampatterns obtained by the proposed algorithm in different iterations. (b) Synthesized beampatterns obtained by different algorithms and the full-wave simulation result of the proposed algorithm.

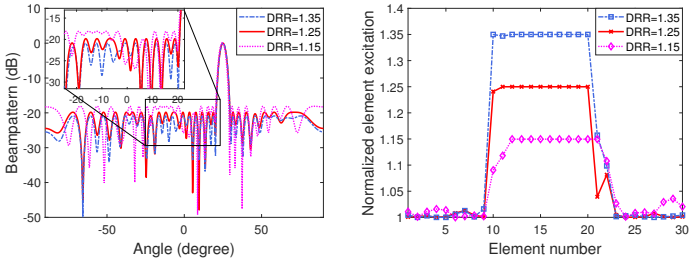

(a) (b)

Fig. 3. Focused beampattern synthesis by the proposed algorithm with different DRR constraints. (a) Synthesized beampatterns obtained with different DRR constraints. (b) Normalized element excitations obtained with different DRR constraints.

where $\beta_m \triangleq \angle(\boldsymbol{w}^H \boldsymbol{a}(\theta_m))$. Then, similar to the formulation (10), we can iteratively update the β_m and $\boldsymbol{w}$. Finally, the problem of shaped beampattern synthesis with DRR constraint can be solved using sequential convex optimization.

IV. Numerical Results

In this section, we conduct representative simulations to show the effectiveness and superiority of the proposed algorithm[1]. We assess the performance of our algorithm by comparing it with the semidefinite relaxation (SDR) algorithm in [13], the iterative approximation algorithm in [15], the auxiliary variables algorithm in [16] and the depth-first algorithm in [17]. For simulations below, the convex optimization problems are solved by CVX toolbox [26], δ is set to 0.1.

A. Focused Beampattern Synthesis With DRR Constraint

In the first example, we use a linear array comprising 30 uniformly spaced isotropic elements, with a spacing of 0.5 λ. The mainlobe axis is $\theta_0 = 25°$. Unless otherwise specified, the DRR is constrained to be below $\varepsilon = 1.25$.

1) Beampattern Comparison: Fig. 2(a) shows the resultant beampatterns of the proposed algorithm at different iterations. One can see that the PSLs are decreased gradually. For the proposed algorithm, the termination condition is satisfied after 6 iterations. The ultimate excitations are provided in Table I, from which the effectiveness of our algorithm in DRR control can be verified. Fig. 2(b) compares the beampatterns obtained by different algorithms. Table II provides the resulting PSLs and running times of different methods, showing that the proposed algorithm obtains the lowest PSL within an acceptable running time. To see the impact of mutual coupling on the proposed algorithm, we conduct a full-wave simulation with patch antennas using CST full-wave simulation software, operating at a center frequency of 2.5 GHz. As shown in Fig. 2(b), the full-wave simulation result of the proposed algorithm is satisfactory.

[1]The MATLAB codes for the proposed algorithm are available online at https://zhangxuejing7.github.io/HomePage/.

TABLE I
The Resulting Excitations for Focused Beampattern Synthesis

i	w_i	i	w_i
1	$0.03280e^{+j0.1290}$	16	$0.04096e^{-j1.1043}$
2	$0.03284e^{-j0.9371}$	17	$0.04096e^{-j2.3552}$
3	$0.03285e^{-j1.5469}$	18	$0.04096e^{+j2.5969}$
4	$0.03278e^{+j1.6382}$	19	$0.04096e^{+j1.1065}$
5	$0.03280e^{+j0.7405}$	20	$0.04096e^{-j0.1507}$
6	$0.03304e^{-j0.0341}$	21	$0.03406e^{-j1.6343}$
7	$0.03320e^{-j2.3317}$	22	$0.03545e^{-j2.7086}$
8	$0.03291e^{-j2.9291}$	23	$0.03292e^{+j1.9001}$
9	$0.03280e^{+j1.8832}$	24	$0.03277e^{+j1.2008}$
10	$0.04066e^{+j0.5772}$	25	$0.03279e^{-j0.6782}$
11	$0.04096e^{-j0.7339}$	26	$0.03281e^{-j1.7149}$
12	$0.04096e^{-j2.1143}$	27	$0.03302e^{+j2.1063}$
13	$0.04096e^{+j2.8979}$	28	$0.03284e^{+j2.8193}$
14	$0.04096e^{+j1.5333}$	29	$0.03277e^{+j0.9734}$
15	$0.04096e^{+j0.1913}$	30	$0.03281e^{-j0.5943}$

TABLE II
The Resulting PSLs and Running Times in The First Example

	Proposed	[13]	[15]	[16]	[17]
PSL (dB)	**-19.82**	-16.50	-17.13	-14.43	-19.16
Running time (s)	**236.33**	74.98	273.32	327.99	5.87

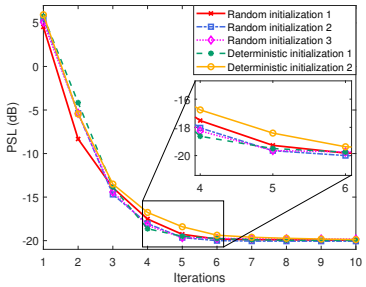

Fig. 4. PSL curves with iterations under different $\bar{\boldsymbol{w}}_0$.

2) Beampattern Synthesis With Different DRR Constraints: To evaluate the influence of DRR on beampattern, Fig. 3(a) presents the results of the proposed algorithm under various DRR constraints. The PSLs obtained with DRR=1.15, DRR=1.25, and DRR=1.35, are -18.11dB, -19.82dB, and -20.88dB, respectively, lower than those of SDR algorithm (-15.13dB, -16.50dB, -18.01dB), the iterative approximation algorithm (-14.97dB, -17.13dB, -17.82dB), the auxiliary variables algorithm (-14.11dB, -14.43dB, -14.52dB) and the depth-first algorithm (-18.01dB, -19.16dB, -20.01dB). It indicates that as the DRR decreases, the achieved PSL increases accordingly. The normalized element excitations obtained using the aforementioned three DRR constraints are depicted in Figure 3(b). One can see that the resulting excitations match the given DRR constraints as desired.

3) Convergence Validation of the Proposed Algorithm: To evaluate the dependence of the proposed algorithm on the initial $\bar{\boldsymbol{w}}_0$, Fig. 4 displays the PSL curves with iterations under different $\bar{\boldsymbol{w}}_0$. For the value of $\bar{\boldsymbol{w}}_0$, we select three sets of random values as well as two sets of deterministic values. The first set of deterministic values is an all-one vector, while the second set has ones for its first half and $e^{j\pi/2}$ for the remaining elements. As can be seen from Fig. 4, for each set of initial $\bar{\boldsymbol{w}}_0$, the obtained PSL decreases with iterations, and converges to approximately -19.90dB after about 8 iterations. This demonstrates that the proposed algorithm does not depend on the selection of initial $\bar{\boldsymbol{w}}_0$ and exhibits good convergence performance.

B. Multi-Beam Scanning With DRR Constraint

In the second example, we assess the performance of the proposed algorithm under multi-beam scanning scenario. We use a non-uniform

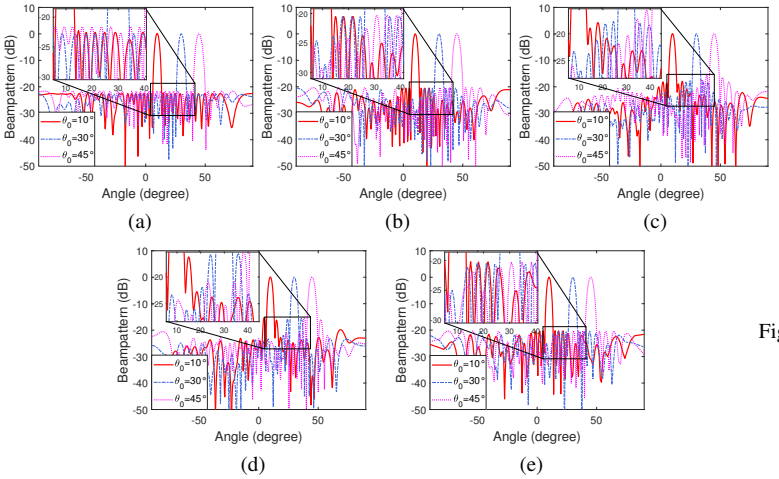

Fig. 5. Beampattern comparison in multi-beam scanning scenario. (a) Beampattern results of the proposed algorithm. (b) Beampattern results of SDR algorithm. (c) Beampattern results of the iterative approximation algorithm. (d) Beampattern results of the auxiliary variables algorithm. (e) Beampattern results of the depth-first algorithm.

TABLE III
THE ELEMENT LOCATIONS OF NON-UNIFORM LINEAR ARRAY IN THE SECOND EXAMPLE

i	$r_i(\lambda)$	i	$r_i(\lambda)$	i	$r_i(\lambda)$	i	$r_i(\lambda)$
1	0.00	10	4.64	19	9.03	28	13.64
2	0.57	11	5.06	20	9.62	29	14.14
3	1.06	12	5.64	21	10.03	30	14.59
4	1.58	13	6.11	22	10.56	31	15.05
5	2.04	14	6.50	23	11.13	32	15.63
6	2.51	15	7.10	24	11.63	33	16.07
7	3.07	16	7.61	25	12.06	34	16.64
8	3.53	17	8.10	26	12.55	35	17.00
9	4.00	18	8.58	27	13.09		

TABLE IV
THE RESULTING PSLS AT DIFFERENT SCANNING ANGLES AND RUNNING TIMES IN THE SECOND EXAMPLE

	Proposed	[13]	[15]	[16]	[17]
PSL at 10° (dB)	**-22.25**	-20.51	-17.92	-15.23	-20.22
PSL at 30° (dB)	**-22.76**	-20.61	-18.02	-15.87	-20.40
PSL at 45° (dB)	**-21.64**	-20.31	-15.57	-15.13	-20.27
Running time (s)	**689.41**	419.58	721.41	833.64	7.23

linear array composed of 35 isotropic elements. The exact element positions $\{r_i\}_{i=1}^{N}$ are outlined in Table III. For simplicity, we consider three beams pointing towards 10°, 30° and 45°, respectively. The DRR is constrained to be below $\varepsilon = 1.60$.

Fig. 5 compares the beampatterns obtained by different methods, while Table IV lists the resulting PSLs at different scanning angles and the running times. Based on the above results, it can be observed that compared to the other methods, the proposed algorithm can achieve a lower PSL under the given DRR constraint.

C. Shaped Beampattern Synthsis With DRR Constraint

In the third example, we assess the performance of the proposed algorithm for shaped beampattern synthesis. We use an uniform linear array composed of 40 isotropic elements. In this case, we constrain the PSL below -15.00dB for sidelobe region $|\theta| \geq 13.5^\circ$. The DRR is constrained to be below $\varepsilon = 3.00$ for the proposed algorithm. Our goal is to minimize the mainbeam ripple level within the mainlobe region $|\theta| \leq 10^\circ$, subject to the above constraints.

Fig. 6 compares the shaped beampattern results obtained by different methods, while Table V lists the relevant data. The proposed

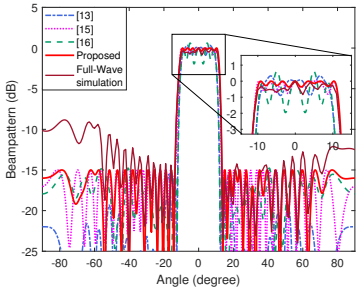

Fig. 6. Shaped beampattern synthesis comparison.

TABLE V
THE RELEVANT DATA IN THE THIRD EXAMPLE

	Proposed	[13]	[15]	[16]
DRR constraint	**3.00**	9.00	6.00	15.00
PSL (dB)	**-15.00**	-15.51	-15.00	-14.77
Ripple level (dB)	**0.36**	1.96	0.80	2.58
Running time (s)	**346.72**	268.37	386.49	637.82

TABLE VI
THE CORRESPONDING ACTIVE VSWR IN THE THIRD EXAMPLE

i	VSWR	i	VSWR	i	VSWR	i	VSWR
1	1.080	11	1.110	21	1.029	31	1.203
2	1.056	12	1.149	22	1.066	32	1.156
3	1.030	13	1.181	23	1.047	33	1.115
4	1.020	14	1.210	24	1.029	34	1.083
5	1.066	15	1.191	25	1.067	35	1.026
6	1.012	16	1.144	26	1.053	36	1.011
7	1.009	17	1.104	27	1.149	37	1.028
8	1.066	18	1.076	28	1.147	38	1.085
9	1.052	19	1.005	29	1.154	39	1.055
10	1.057	20	1.007	30	1.182	40	1.139

algorithm can be observed to not only satisfy the PSL constraint but also demand a relatively short running time, while attaining the minimal ripple level even under the strictest DRR constraint. On the other hand, since the requirement of additional correction, the resulting PSL of the auxiliary variables algorithm is slightly raised. The above results confirm the effectiveness and superiority of the proposed algorithm. With the same antenna configuration as in the first example, we conduct a full-wave simulation, and the result is presented in Fig. 6. Although there is an increase in sidelobe level especially in the angular regions that are far from the mainlobe, the full-wave simulation result is generally acceptable. Accordingly, the active voltage standing wave ratio (VSWR) is shown in Table VI for reference. Also, note that the depth-first algorithm is unable to solve the shaped beampattern synthesis problem and consequently not shown in this scenario.

V. CONCLUSIONS

In this paper, we have proposed a sequential convex optimization algorithm for beampattern synthesis with DRR constraint. The DRR constraint has been reformulated and simplified, enabling the utilization of sequential convex optimization to address the non-convex beampattern synthesis problem. The proposed algorithm has proven to be not only easy to implement, but also highly effective on focused or shaped beampatterns. Both theoretical and simulation results have confirmed that the proposed algorithm does not rely on the initial setting and exhibits good convergence performance. Representative simulations have been conducted to show the effectiveness and superiority of the proposed algorithm.

REFERENCES

[1] F. J. Ares-Pena, J. A. Rodriguez-Gonzalez, E. Villanueva-Lopez and R. Guinvarch, "Genetic algorithm in the design and optimization of antenna array patterns," *IEEE Trans. Antennas Propag.*, vol. 47, no. 3, pp. 506-510, 1999.

[2] M. M. Khodier and C. G. Christodoulou, "Linear array geometry synthesis with minimum sidelobe level and null control using particle swarm optimization," *IEEE Trans. Antennas Propag.*, vol. 53, no. 8, pp. 2674-2679, 2005.

[3] S. K. Mahto and A. Choubey, "A novel hybrid IWO/WDO algorithm for interference minimization of uniformly excited linear sparse array by position-only control," *IEEE Antennas Wireless Propag. Lett.*, vol. 15, pp. 250-254, 2016.

[4] O. M. Bucci and S. Perna, "A deterministic two dimensional density taper approach for fast design of uniform amplitude pencil beams arrays," *IEEE Trans. Antennas Propag.*, vol. 59, no. 8, pp. 2852-2861, 2011.

[5] W. P. M. N. Keizer, "Synthesis of thinned planar circular and square arrays using density tapering," *IEEE Trans. Antennas Propag.*, vol. 62, no. 4, pp. 1555-1563, 2014.

[6] G. Buttazzoni and R. Vescovo, "Reducing the sidelobe power pattern of linear broadside arrays by refining the element positions," *IEEE Antennas Wireless Propag. Lett.*, vol. 17, no. 8, pp. 1464-1468, 2018.

[7] R. C. Nongpiur and D. J. Shpak, "Synthesis of linear and planar arrays with minimum element selection," *IEEE Trans. Signal Process.*, vol. 62, no. 20, pp. 5398-5410, 2014.

[8] B. Fuchs and S. Rondineau, "Array pattern synthesis with excitation control via norm minimization," *IEEE Trans. Antennas Propag.*, vol. 64, no. 10, pp. 4228-4234, 2016.

[9] G. Buttazzoni and R. Vescovo, "Density tapering of linear arrays radiating pencil beams: A new extremely fast Gaussian approach," *IEEE Trans. Antennas Propag.*, vol. 65, no. 12, pp. 7372-7377, 2017.

[10] B. Fuchs, "Application of convex relaxation to array synthesis problems," *IEEE Trans. Antennas Propag.*, vol. 62, no. 2, pp. 634-640, 2014.

[11] S. Lei, Y. Yang, H. Hu, Z. Zhao, B. Chen and X. Qiu, "Power gain optimization method for wide-beam array antenna via convex optimization," *IEEE Trans. Antennas Propag.*, vol. 67, no. 3, pp. 1620-1629, 2019.

[12] R. Vescovo, "Consistency of constraints on nulls and on dynamic range ratio in pattern synthesis for antenna arrays," *IEEE Trans. Antennas Propag.*, vol. 55, no. 10, pp. 2662-2670, 2007.

[13] B. Fuchs and S. Rondineau, "Array pattern synthesis with excitation control via norm minimization," *IEEE Trans. Antennas Propag.*, vol. 64, no. 10, pp. 4228-4234, 2016.

[14] G. Strang, *Introduction to Linear Algebra*. New York, USA: Wellesley Cambridge. Press, 2009.

[15] S. Lei, P. Tang, B. Chen, J. Tian, W. Yang and X. Qiu, "Power-gain pattern synthesis of array antenna with dynamic range ratio restriction," *IEEE Antennas Wireless Propag. Lett.*, vol. 18, no. 12, pp. 2691-2695, 2019.

[16] X. Fan, J. Liang, Y. Jing, H. C. So, Q. Geng and X. Zhao, "Sum/Difference pattern synthesis with dynamic range ratio control for arbitrary arrays," *IEEE Trans. Antennas Propag.*, vol. 70, no. 3, pp. 1940-1953, 2022.

[17] K. Vodvarka, M. J. Bellotti and M. Vucic, "Synthesis of l_1 pencil beams with constrained sidelobe level and dynamic range ratio," *Proc. 2022 16th European Conf. Antennas Propag.*, pp. 1-5, 2022.

[18] Z. Lin, H. Hu, S. Lei, R. Li, J. Tian and B. Chen, "Low-sidelobe shaped-beam pattern synthesis with amplitude constraints," *IEEE Trans. Antennas Propag.*, vol. 70, no. 4, pp. 2717-2731, 2022.

[19] M. Vucic, M. J. Bellotti and K. Vodvarka, "Synthesis of flat-top beampattern with minimax sidelobes and constrained dynamic range ratio," *Proc. 2023 IEEE Int.Symp. Antennas Propag. USNC/URSI Nat. Radio Sci. Meeting.*, pp. 385-386, 2023.

[20] M. Cheng, Q. Wu, C. Yu, H. Wang and W. Hong, "Synthesis of a thinned prephased electronically steered phased array using excitation control of both the small amplitude dynamic range ratio and low-resolution phase," *IEEE Trans. Antennas Propag.*, vol. 72, no. 1, pp. 600-613, 2024.

[21] G. Buttazzoni and R. Vescovo, "Power synthesis for reconfigurable arrays by phase-only control with simultaneous dynamic range ratio and near-field reduction," *IEEE Trans. Antennas Propag.*, vol. 60, no. 2, pp. 1161-1165, 2012.

[22] M. Comisso and R. Vescovo, "Fast co-polar and cross-polar 3D pattern synthesis with dynamic range ratio reduction for conformal antenna arrays," *IEEE Trans. Antennas Propag.*, vol. 61, no. 2, pp. 614-626, 2013.

[23] O. M. Bucci, G. Mazzarella and G. Panariello, "Reconfigurable arrays by phase-only control," *IEEE Trans. Antennas Propag.*, vol. 39, no. 7, pp. 919-925, 1991.

[24] R. Vescovo, "Reconfigurability and beam scanning with phase-only control for antenna arrays," *IEEE Trans. Antennas Propag.*, vol. 56, no. 6, pp. 1555-1565, 2008.

[25] Q. Li, L. Huang, H. C. So, H. Xue and P. Zhang, "Beampattern synthesis for frequency diverse array via reweighted ℓ_1 iterative phase compensation," *IEEE Trans. Aerosp Electron Syst.*, vol. 54, no. 1, pp. 467-475, 2018.

[26] M. Grant and S. Boyd, "CVX: Matlab software for disciplined convex programming, version 2.1," *http://cvxr.com/cvx*, 2015.